Journal of Power Sources 235 (2013) 265–273

Contents lists available at SciVerse ScienceDirect

Journal of Power Sources

journal homepage: www.elsevier.com/locate/jpowsour

On the use of lithium vanadium phosphate in high power devices

N. Böckenfeld, A. Balducci*

Westfälische Wilhelms Universität, Institut für Physikalische Chemie-MEET, Corrensstr. 28/30, 48149 Münster, Germany

HIGHLIGHTS

- Lithium vanadium phosphate is attractive for the realization of high power devices.
- Lithium-ion capacitors containing lithium vanadium phosphate display high energy and power.
- Lithium-ion batteries containing lithium vanadium phosphate as the only active material display promising performance.

ARTICLE INFO

Article history:
Received 1 October 2012
Received in revised form
5 December 2012
Accepted 3 February 2013
Available online 16 February 2013

Keywords:
LVP
Anode
Cathode
Lithium batteries
Lithium-ion capacitors

ABSTRACT

Lithium vanadium phosphate can be conveniently used as cathodic and anodic material, and it displays high performance during charge–discharge tests carried out at high current densities. Using a sol–gel method two different LVP samples, having different carbon content, were synthesized. The lithium diffusion coefficient as well as the rate performance of the electrodes was investigated. The electrodes were used for the realization of three different electrochemical devices: a LIC, a hybrid device containing LVP as cathode and a LVP-based lithium-ion battery. The performance of all devices was investigated in terms of cycling stability, and their energy and power were evaluated. The results of these tests indicate LVP as an interesting and flexible candidate for the realization of high power system.

1. Introduction

Lithium-ion batteries (LIB) are at present the most advanced secondary batteries due to their high energy as well as power capabilities [1]. With the aim to further improve the performance of these electrochemical devices, several electrode materials have been proposed and investigated in the last years [2–6]. Among them, lithium vanadium phosphate ($Li_3V_2(PO_4)_3$, LVP) is currently considered as one of the most interesting, and an increasing number of work is now focusing on the synthesis and on the application of this material in LIB.

LVP displays a monoclinic structure ($P2_1/n$) consisting of a three-dimensional framework with distorted VO_6-octahedra and PO_4-tetrahedra sharing corner with each other [7]. So far several synthetic routes, including solid-state reaction [8–10], carbo-thermal reduction [7,11–13], hydrothermal [14,15] and sol–gel synthesis [15–19] as well as rheological-phase reaction [20] have been used for the synthesis of LVP. In all these preparation methods it is necessary to carry out the indispensable reduction process from the V^{+5} precursor to the V^{+3} product by either addition of hydrogen to the reaction atmosphere during the heat treatment, or addition of reductive sugars or carboxylic acids like glucose, sucrose, maltose, oxalic acid and citric acid to the precursor mixture [12,15,21–23]. It is important to note that most of these organic precursors decompose under protective gas atmosphere during the heat treatment. For this reason, most of these syntheses lead to the formation of carbon-coated LVP particles. Such coating is considered of particular importance since it considerably improves the electronic conductivity of LVP [22].

LVP belongs to the category of the amphoteric materials and for this reason it can be conveniently used as anodic and cathodic material. Initially, most of the investigations on LVP focused on the use of this material as cathode for LIBs. Several studies showed that a complete and reversible extraction of the three lithium ions is possible from LVP [7]. The extraction of lithium occurs at 3.65 V vs. Li/Li^+ (0.5 Li), 3.75 vs. Li/Li^+ (0.5 Li), 4.15 vs. Li/Li^+ (1 Li) and 4.65 V vs. Li/Li^+ (1 Li). In the case of full delithiation of the host framework a theoretical capacity of 197 mAh g^{-1} is reached. More recently, also

* Corresponding author.
E-mail address: andrea.balducci@uni-muenster.de (A. Balducci).

0378-7753/$ – see front matter © 2013 Elsevier B.V. All rights reserved.
http://dx.doi.org/10.1016/j.jpowsour.2013.02.019

the use of LVP as anode has been considered. Some studies indicated that LVP is able to reversibly take and release lithium in a series of two-phase transition processes between 3.0 and 1.6 V vs. Li/Li^+, and a single-phase process between 1.6 and 0.0 V vs. Li/Li^+ [11,24]. The same studies also highlighted that carbon-coating and carbon residues might generate irreversible capacity, limiting the performance of LVP-based anodes.

One interesting aspect related to the use of the amphoteric LVP is that this material provides the opportunity to design a lithium-ion battery containing only one kind of active material. Since lithium extraction occurs above 3.5 V vs. Li/Li^+, while lithium intercalation takes place below 2 V vs. Li/Li^+, a LVP-based LIB might display a maximum cell voltage in the order of 4 V. Several publications showed that LVP electrodes (both anode and cathode) display high performance during test carried out at high current densities [22,25,26]. Therefore, a LVP-based LIB battery should also be able to display good power performance.

Furthermore, it is very interesting to note that the superior performance of LVP during tests at high current densities makes this material an attractive candidate for the realization of high power electrochemical devices. For example, LVP could be very attractive for the realization of lithium-ion capacitors (LIC). Usually, the term lithium-ion capacitor is used to describe a hybrid device containing graphite or soft carbon as anode and activated carbon (AC) as cathode [27–29]. However, such configuration could be also realized using a different anode, e.g. LVP, instead of graphite. Moreover, LVP could be very interesting also for the realization of a hybrid device with reversed design compared to the standard LIC, where a LVP-based cathode is coupled with an AC anode. Several examples of this kind of device have been reported in literature and due to their performance the interest on these hybrid systems constantly increased in the last years [30–35].

To the best of our knowledge the use of LVP in high power devices has never been investigated. Nevertheless, taking into account the unique properties of this material, such study could offer new and interesting information about the use of LVP in electrochemical devices. With the aim to investigate this aspect, LVP particles containing different carbon content were synthesized using a sol–gel method and, after their structural and morphological characterization, they were used for the realization of composite electrodes. Initially, the lithium diffusion coefficient and the rate performance of the prepared electrodes were investigated. Afterward, the electrodes were used for the realization of a LIC, a hybrid device containing LVP as cathode and a LVP-based lithium-ion battery. The performance of all devices was investigated in terms of cycling stability and their energy and power were evaluated.

2. Experimental

2.1. Synthesis

Two different LVP samples were prepared via a sol–gel method using NH_4VO_3, $LiCH_3COO$ and $NH_4H_2PO_4$ (in a molar ratio of 2:3:3) as precursor. Citric acid or a mixture of citric and oxalic acid ($V:Li:PO_4:CA = 2:3:3:10$ or $V:Li:PO_4:CA:OA = 2:3:3:2:6$) was used as reducing and chelating agent. Initially, NH_4VO_3 and the reducing agent (either citric acid or a mixture of citric–oxalic acid) were dissolved in deionized water at 80 °C. Afterward, a solution containing $LiCH_3COO$ and $NH_4H_2PO_4$ was prepared at 80 °C and added to the first one. The obtained solution was stirred at 80 °C in order to obtain a dark green gel, which was dried for 24 h under ambient atmosphere in an oven at 80 °C. The gel precursor was grinded with an agate mortar, transferred to a tube furnace and sintered under constant flow of Argon at 300 °C for 4 h with a heating rate of 5 °C min^{-1}. The resulting precursor was reground and then sintered under constant flow of Argon at 750 °C for 12 h with a heating rate of 10 °C min^{-1}. In the following, the LVP sample obtained using citric acid will be indicated as LVP/CA, while the LVP sample obtained using the mixture of citric acid and oxalic acid will be indicated as LVP/CA + OA.

The lithium, vanadium and phosphorus content of the two LVP samples were determined by the inductively coupled plasma optical emission spectrometry (ICP-OES, SPECTRO ARCOS, Ametek, Germany). The crystalline structure was characterized by X-ray diffraction (XRD) using the Cu Kα radiation on the Bruker D8 Advance (Germany) in the 2θ range from 10° to 60°. Lattice parameters were determined by Rietveld refinement with TOPAS (Bruker) software. The carbon and hydrogen content of the samples was evaluated by elementary CHN combustion analysis.

2.2. Electrode preparation and characterization

Composite electrodes containing LVP as active material were prepared using a casting process similar to that reported in Ref. [36]. The composition of the dry electrodes was 85% LVP, 10% conducting agent (Super C65, TIMCAL) and 5% binder (Polyvinylidene fluoride, PVdF). The electrodes containing LVP/CA as active material were coated on etched aluminum foil (5 wt.% KOH, 60 °C, 30 s). The electrodes containing LVP/CA + OA as active material were coated on dendritic copper foil. The electrode area was 1.13 cm^2. The electrode mass loading was about 0.8 mg cm^{-2}. The electrode density was 1.2 g cm^{-3}. Composite electrodes containing activated carbons (AC) were prepared using a casting process similar to that reported in Ref. [36]. The composition of the dry electrodes was 85% AC (DLC Super 30, Norit), 10% conducting agent (Super C65, TIMCAL) and 5% binder (Sodium carboxymethyl-cellulose, Dow Wolff Cellulosics, Walocel CRT 2000 PPA 12). The electrode area was 1.13 cm^2. The electrode mass loading comprised 2–4 mg cm^{-2}. The electrode density was 0.55 g cm^{-3}.

Electrochemical tests were carried out in Swagelok®-type 3-electrodes cells, which were assembled in an argon-filled glove box ($H_2O < 1$ ppm, $O_2 < 1$ ppm). For all experiments, a Whatman GF/D glass microfiber filter of 675 μm in thickness and 12 mm in diameter was used as a separator. The separator was drenched with 120 μL of 1 M $LiPF_6$ in ethylene carbonate/dimethyl carbonate (EC/DMC) 1:1.

The composite electrodes containing LVP/CA and LVP/CA + OA as active materials were initially tested in half-cell configuration, using metallic lithium as counter and reference electrodes. Cyclic voltammetries (CV) were performed using a VMP multichannel potentiostatic–galvanostatic system (Biologic Science Instrument, France). In the case of the composites electrodes containing LVP/CA, the CV were carried out in the voltage range from 3.0 to 4.3 V vs. Li/Li^+. In the case of the composites electrodes containing LVP/CA + OA the CV were carried out in the voltage range from 3.0 to 0.0 vs. Li/Li^+. For both electrodes four different scan rates (0.05, 0.1, 0.2 and 0.5 mV s^{-1}) were used. Constant current (CC) tests were performed applying charge–discharge currents ranging from to C/2 to 10 C. In the case of the electrodes containing LVP/CA a nominal capacity of 133 mAh g^{-1} was used for the calculation of the current densities. In the case of the electrodes containing LVP/CA + OA, a nominal capacity of 550 mAh g^{-1} was considered [11,24]. Five full charge–discharge cycles were carried out for each considered C-rate. After the C-rate test, 100 cycles at a current corresponding to 1 C were carried out. The cut-off potentials used for the CC tests were identical to that used for the CV test.

Three different electrochemical devices were assembled using the LVP-based electrodes. In the first device, indicated as hybrid device, a LVP/CA electrode was used as cathode and combined with

an AC-based anode. The weight ratio between the active material of LVP/CA and AC was (1:3.5 wt.). During the cycling, the potential of the LVP/CA electrode was limited to 3.0–4.3 V vs. Li/Li^+, and the lower cell voltage was limited to 0 V. In the second device, indicated as LIC, a LVP/CA + OA electrode was used as anode and it was combined with an AC-based cathode. The weight ratio between the active material LVP/CA + OA and AC was (1:2.35 wt.). Before the cycling a prelithiation process of the LVP/CA + OA anode was carried out by using the lithium metal reference as counter electrode. The prelithiation was done by charge/discharging the LVP/CA + OA anode three times in the voltage range from 0 to 3.0 V vs. Li/Li^+ at a current of C/2 and a final lithiation step at C/2 which ended at a potential limit of 0 V vs. Li/Li^+. During the cycling, the excursion of the LVP/CA + OA electrode was limited between 0 and 1.5 V vs. Li/Li^+, and the lower cell voltage was limited to 0 V. For both devices 1000 CC full charge–discharge cycles using a current corresponding to 10 C were initially carried out. In the case of the hybrid device (containing LVP/CA as cathode) a nominal capacity of 133 mAh g^{-1} was used for the calculation of the current density corresponding to 1 C. In the case of the LIC (containing LVP/CA + OA as anode), a nominal capacity of 550 mAh g^{-1} was considered. After the CC test, both devices were subject to a C-rate test carried out applying currents corresponding to 1 C, 2 C, 5 C, 10 C, 20 C, 50 C and 100 C. Ten full charge–discharge cycles were carried out for each considered C-rate. The third electrochemical device considered in this work was a lithium-ion battery containing the LVP/CA electrode as cathode and LVP/CA + OA electrode as anode. The weight ratio between the anode/cathode active materials was (1:2 wt.). During the CC test the potential of the LVP/CA + OA anode was controlled and limited to a range of 0–3.0 V vs. Li/Li^+. The potential of the full-cell as well as the anode was monitored, while the cathode potential was derived from those values. Initially, the LIB was subject to a C-rate test. For the determination of the C-rate, the nominal specific capacity of the LVP/CA + OA anode (550 mAh g^{-1}) was considered. After the C-rate test 100 cycles at a current corresponding to 1 C were carried out.

All values of specific capacity calculated for the three devices and reported in the following pages are based on the sum of the active materials of both electrodes (anode and cathode). The average energy and the power of the three devices were calculated as reported in Ref. [37].

All CC test (for half cells as well as for the three full cells) were carried out at 20 °C using a Maccor series 4000 battery tester. All voltage quoted in the following pages refer to the Li/Li^+ couple.

3. Results and discussion

Fig. 1a shows the XRD patterns and the SEM images of LVP particles synthesized by a sol–gel method using citric acid (LVP/CA) or a mixture of citric acid and oxalic acid (LVP/CA + OA) as the reducing agent. As shown in Fig. 1a, all diffraction peaks observed for samples LVP/CA and LVP/CA + OA could be attributed to the monoclinic structure ($P2_1/n$) of LVP. As indicated in Table 1, the dimensions and volume of the unit cell were almost identical for both samples, indicating that both synthetic procedures lead to compounds with an identical crystal structure. However, as showed in the SEM images, the use of different reducing agents modifies significantly the morphology of the samples. As shown in Fig. 1b, the use of citric acid leads to the formation of LVP particles with a size in the order of 1 μm. These particles are "dispersed" between large amounts of carbonaceous residues having a size in the order of 10 μm. These carbonaceous residues are formed by the decomposition of the citric acid, which took place during the heat treatment of the precursor [18]. As reported in Table 1, the carbon content of the LVP/CA sample was equal to 25.3%. The use of a

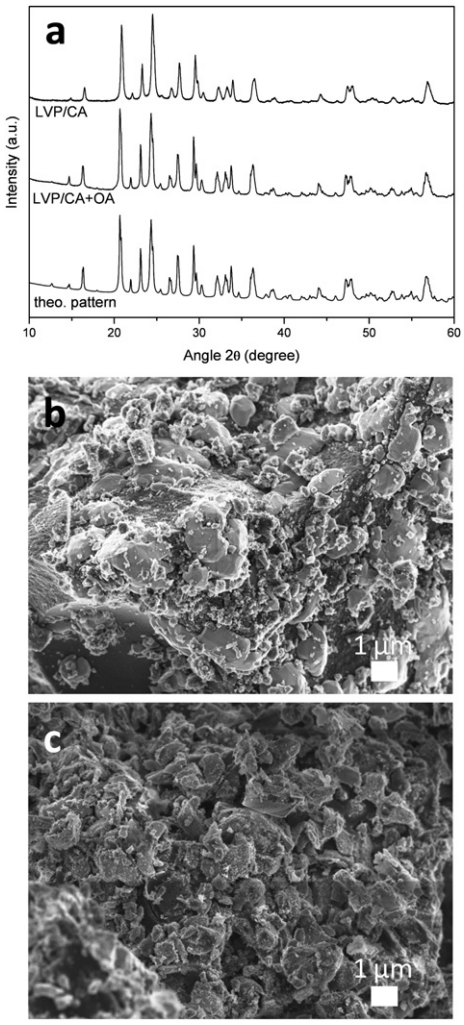

Fig. 1. (a) XRD patterns of LVP/CA and LVP/CA + OA samples in a 2θ range from 10 to 60°. For comparison the ideal pattern based on single-phase LVP (ICSD No. 96962) is also depicted. (b) SEM image of LVP/CA powder. (c) SEM image of LVP/CA + OA powder.

mixture of citric acid and oxalic acid as the reducing agent leads to the formation of LVP in the order of 1–2 μm (Fig. 1c). Moreover, the carbon content of the LVP/CA–OA sample was equal to 7.5% (see Table 1), and no big agglomerates of carbon particles were observed. Most likely, the lower content of carbon is due the decomposition of the oxalic acid (which displays high oxygen content) during the heat treatment applied for the synthesis [15]. Such decomposition process might affect both the LVP and carbon morphology [18].

Table 1
Characteristics of LVP/CA and LVP/CA + OA powders: lattice parameters, cell volume (from Rietveld refinement of the XRD diffractogram); carbon content based on CHN analysis results; ratio between Li, V and P based on ICP-OES data.

	LVP/CA	LVP/CA + OA
a (Å)	8.585	8.606
b (Å)	8.576	8.592
c (Å)	12.014	12.037
β ( )	90.40	90.61
V_{cell} (Å^3)	884.56	890.4
Space group	$P2_1/n$	$P2_1/n$
Carbon content (%)	25.3	7.5
Hydrogen content (%)	<0.5	<0.5
L:V:P ratio	3:1.99:2.94	3:1.99:2.85

As mentioned in the Introduction, LVP can be used as cathodic as well as anodic material. However, when used as anodic material, the presence of carbon residues need to be carefully considered since these residues might generate irreversible capacity, limiting the electrode performance. Taking into account this point, and considering the characteristics of the two LVP samples described above, we therefore investigate the performance of the sample LVP/CA as cathode, and those of the samples LVP/CA–OA as anode.

Fig. 2a shows the voltammetric profiles of the LVP/CA electrode in the potential range from 3.0 to 4.3 V obtained using scan rates ranging from 0.05 to 0.5 mV s^{-1}. In this potential range two lithium ions are extracted from the structure. The oxidation peaks A1 (3.6 V), A2 (3.685 V) and the reduction peaks C1 (3.567 V), C2 (3.651 V) correspond each to extraction/insertion of 0.5 Li. The third pair of oxidation and reduction peaks A3 (4.1 V) and C3 (4.051 V) represents the extraction/insertion of 1 Li. Although perfectly reversible, a minor difference can be observed between the extraction of the first and the second lithium. At a scan rate of 0.05 mV s^{-1}, the potential difference (ΔV) between the peaks A1–C1 and A2–C2 is 0.033 V and 0.034 V, respectively. These values are very similar (see also Table 2), indicating a similar diffusion for both processes. The potential difference between A3–C3 is slightly higher (0.049 V), indicating a slightly slower diffusion process.

Fig. 2b shows the voltammetric profiles of the LVP/CA + OA electrode in the potential range from 3.0 to 0.0 V. Also in this case, the experiments were conducted using scan rates ranging from 0.05 to 0.5 mV s^{-1}. As mentioned in the Introduction, when used as anode, LVP is able to reversibly take and release lithium in a series of two-phase transition processes between 3.0 and 1.6 V vs. Li/Li^+, and a single-phase process between 1.6 and 0.0 V vs. Li/Li^+ [11,24]. As shown in the figure, when a scan rate of 0.05 mV s^{-1} was used, four oxidation and four reduction peaks could be distinguished. However, when the scan rate was increased, only three peaks were observed. It is interesting to note that while the ΔV between the peaks A1–C1 and A2–C2 was rather similar (0.040 V and 0.043 V, respectively, see also Table 2), the ΔV between the peaks A3–C3 was three times higher, indicating a limited diffusion process.

In order to quantitatively evaluate the lithium diffusion processes in the LVP electrodes, the peaks current (i_p) at different scan rates were plotted against the square root of the scan rate ($\nu^{1/2}$) [23,24,38,39]. As shown in Fig. 3c and d, a linear relationship between i_p and $\nu^{1/2}$ was observed for both electrodes. As already reported in literature, such behavior indicates the presence of a diffusion limited intercalation process. Assuming that this kind of process is taking place on the electrodes, the Randles–Sevcik equation, derived for semi-infinite diffusion processes, can be applied to both materials to calculate the lithium diffusion constant D_{Li^+} [40]:

$$i_p = \left(2.69 \times 10^{-5}\right) n^{3/2} A D_{Li^+}^{1/2} C_{Li} \nu^{1/2} \quad (1)$$

In equation (1) i_p is the maximum peak current (A), n is the charge-transfer number, A is the contact area between LVP electrode and electrolyte (geometric area as approximation, 1.13 cm^2), C_{Li} is the concentration of lithium ions in the LVP material (3.7×10^{-3} mol cm^{-3}, calculated from the volume of the unit cell of LVP) and ν is the potential scan rate (V s^{-1}). It is important to take into account that the equation (1) is not designed to describe the occurring two-phase process, where diffusion through the phase boundaries and two phases with different lithium content influence the overall lithium diffusion. Nevertheless, the values obtained for

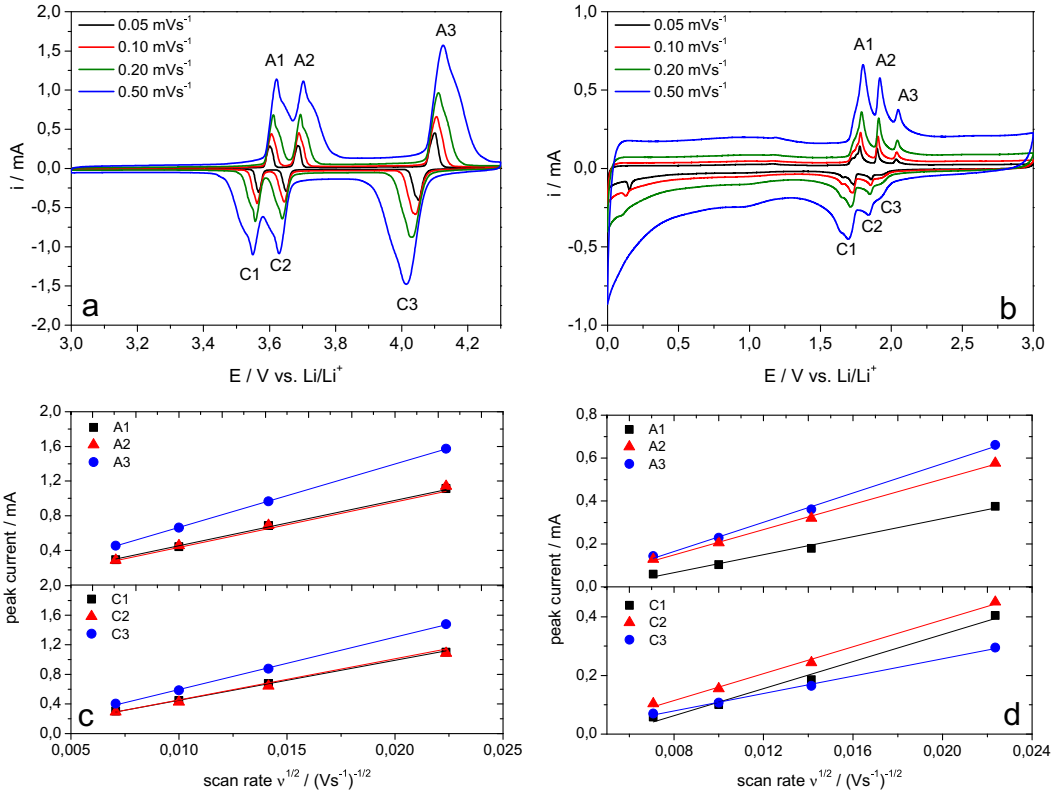

Fig. 2. (a) CVs of LVP/CA electrode in the potential range from 3.0 to 4.3 V vs. Li/Li^+ at scan rates ranging from 0.05 to 0.5 mV s^{-1}; (b) plot of peak currents (i_p) versus square root of the scan rate ($\nu^{1/2}$) for the LVP/CA electrode. (c) CVs of LVP/CA + OA electrode in the potential range from 0.0 to 3.0 V vs. Li/Li^+ at scan rates ranging from 0.05 to 0.5 mV s^{-1}; (d) plot of peak currents (i_p) versus square root of the scan rate ($\nu^{1/2}$) for the LVP/CA + OA electrode.

Table 2
Potential differences of oxidation and reduction peaks for the LVP/CA and LVP/CA + OA electrodes obtained during cyclic voltammetry carried out at a scan rate of 0.05 mV s^{-1}.

ΔV (V)	LVP/CA	LVP/CA + OA
Δ(A1 − C1)	0.033	0.040
Δ(A2 − C2)	0.034	0.043
Δ(A3 − C3)	0.049	0.112

this calculation might help to classify the processes and can be treated as apparent diffusion constants, as they are the result of the aforementioned factors. Taking this point into account, we therefore calculate the lithium diffusion on the two LVP electrodes, and the results of this calculation are reported in Table 3. As indicated in the table, in the case of the LVP/CA electrode the A1–C1 and A2–C2 peak couples show diffusion constants in the order of 2×10^{-8} cm^2 s^{-1}. It is important to note that both D_{Li^+} values are very high for a cathode material, confirming the high-rate capability of LVP. In contrast to this high D_{Li^+} values the lithium diffusion constants calculated for the A3–C3 peaks are significantly lower, about 4×10^{-9} cm^2 s^{-1}. In the case of the LVP/CA + OA electrode, the A1–C1 peak couple shows diffusion constants of about $4–9 \times 10^{-10}$ cm^2 s^{-1} while the A2–C2 peak couple values of $2–7 \times 10^{-10}$ cm^2 s^{-1}. As shown in Table 3, these values are rather different compared to that observed for the A3–C3 redox process, which shows values for the diffusion constant of $8–30 \times 10^{-11}$ cm^2 s^{-1}. This marked difference appears in line with the relatively large ΔV (0.112 V) observed from the CV profiles. These values are in good agreement with the results of previous investigations, and show a clear trend of lithium diffusion constants with variation in potential value respectively lithium content [23,24].

Fig. 3 shows the electrochemical performance of the LVP electrodes (cathode and anode) obtained during CC tests carried out at different current densities as well as the cycling stability of the same electrodes during CC test carried out at 1 C. As shown, the LVP/CA cathode is able to deliver 110 and 100 mAh g^{-1} at C/2 and 10 C, respectively (Fig. 3a). These results clearly point out the excellent performance of LVP electrode during tests at high current density. Furthermore, the stability test indicated that this electrode is able to retain 94.7% of its initial capacity after 100 full charge–discharge cycles at 1 C (Fig. 3b). The voltage curve of the first cycle at 1 C is reported in Fig. 3c. As shown, it displays the three

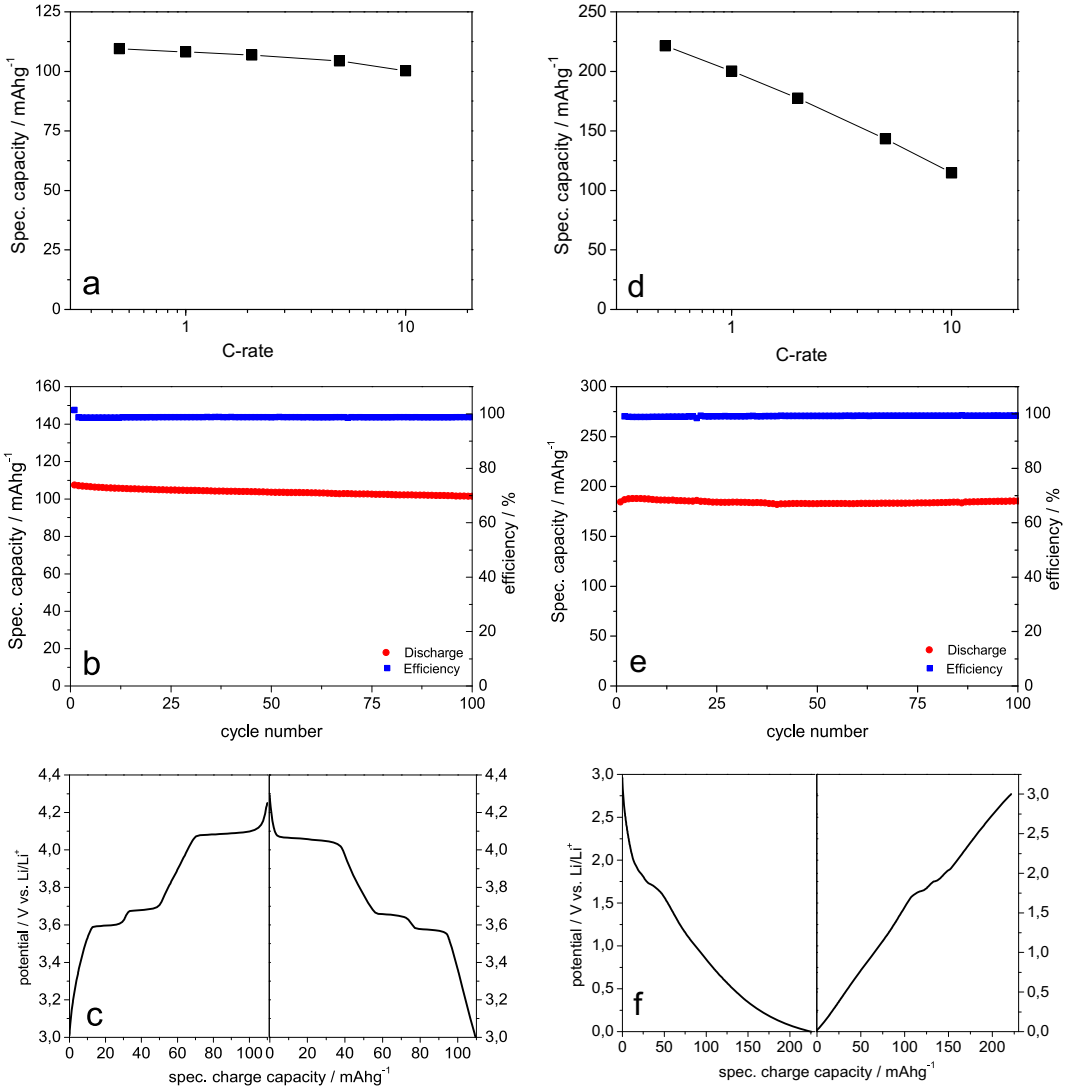

Fig. 3. (a) Rate performance, (b) specific discharge capacity and coulombic efficiency and (c) charge–discharge voltage profile (1st cycles) as obtained from CC tests at 1 C for the LVP/CA electrode cycled in the potential range from 3.0 to 4.3 V vs. Li/Li. (d) Rate performance, (e) specific discharge capacity and coulombic efficiency and (f) charge–discharge voltage profile (1st cycles) as obtained from CC tests at 1 C for the LVP/CA + OA electrode cycled in the potential range from 0.0 to 3.0 V vs. Li/Li.

Table 3
Diffusion coefficients calculated from cyclic voltammetry carried out at a scan rates from 0.05 to 0.5 mV s^{-1} for LVP/CA and LVP/CA + OA electrodes.

D_{Li^+} (cm^2 s^{-1})	LVP/CA (3–4.3 V)	LVP/CA + OA (0–3.0 V)
A1	1.84×10^{-8}	9.19×10^{-10}
A2	1.96×10^{-8}	6.87×10^{-10}
A3	4.25×10^{-9}	3.47×10^{-10}
C1	1.74×10^{-8}	4.16×10^{-10}
C2	1.73×10^{-8}	1.74×10^{-10}
C3	3.96×10^{-9}	8.16×10^{-11}

plateaus, which are expected in this potential region, at 3.65 (0.5 Li), 3.75 (0.5 Li) and 4.15 V vs. Li/Li^+ (1 Li) and correspond to the lithiation/delithiation of two lithium ions. The LVP/CA + OA anode material displays 221 and 115 mAh g^{-1} at C/2 and 10 C, respectively (Fig. 3d). Although this rate performance is not as high as for the LVP/CA cathode, the results of this test indicate that also LVP/CA + OA displays promising performance during tests carried out at high current density. Moreover, in the case of this electrode, it is important to consider that the assumed nominal capacity (and therefore the applied currents) were about four times higher with respect to the LVP/CA electrode. During the constant-current cycling, which was carried out after to the C-rate test, the LVP/CA + OA maintained 98.7% of its initial capacity after 100 cycles carried out at 1 C (Fig. 3e), indicating that also this electrode displays high cycling stability. As shown in Fig. 3f, the typical voltage profile of LVP-anode was observed for this electrode [11].

The results reported above clearly showed that the both, LVP/CA and LVP/CA + OA electrodes displayed high performance during tests carried out at high current densities as well as high cycling stability. For this reason, both of them could be considered for the realization of high power devices. As mentioned in the introduction, two different systems could be realized using the LVP electrodes. The first one is a hybrid device containing a LVP cathode combined with an AC anode. The second one is a LIC containing an AC cathode combined with a LVP anode.

Fig. 4 shows the performance displayed by a hybrid system in which a LVP/CA cathode was combined with AC anode. Initially, with the goal to evaluate the capacity retention of the device, 1000 full charge–discharge cycles at a current corresponding to 10 C (based on the LVP/CA electrode nominal capacity) were conducted. As shown in Fig. 4a, the devices displayed at the beginning of the cycling a specific capacity of 23 mAh g^{-1} (referred to the total active material). During all cycling the coulombic efficiency of the charge–discharge process was higher than 99.5%, and the capacity retention after 1000 full charge–discharge cycles was 87%. The maximum cell voltage of this hybrid device is 2.45 V and, as shown in Fig. 4b, (depicting the 10th cycle of the charge–discharge test), the LVP/CA electrode is working in the potential range of 3.0–4.3 V, while the AC-based electrode in a potential range from 3.0 to about 1.8 V. The three plateaus of the LVP/CA cathode material can be easily distinguished indicating that even under high current density, and without a lithium-containing counter electrode, the material provides fully reversible lithium intercalation. As expected, the voltage profile of active carbon anode shows the typical triangular shape caused by the pure capacitive behavior which relates to ion double-layer capacitance [36]. As shown in Fig. 4c, this hybrid device displays very promising performance also at higher current densities (it is important to note that these tests were carried out after the cycling at 10 C). As a matter of fact, when a current corresponding to 1 C is applied the device delivers a capacity of 22.1 mAh g^{-1}. When the current is increase up to 100 C, the device is able to provide 9.5 mAh g^{-1}, which is more than 40% of the capacity observed at 1 C. Clearly, the performance of this system could

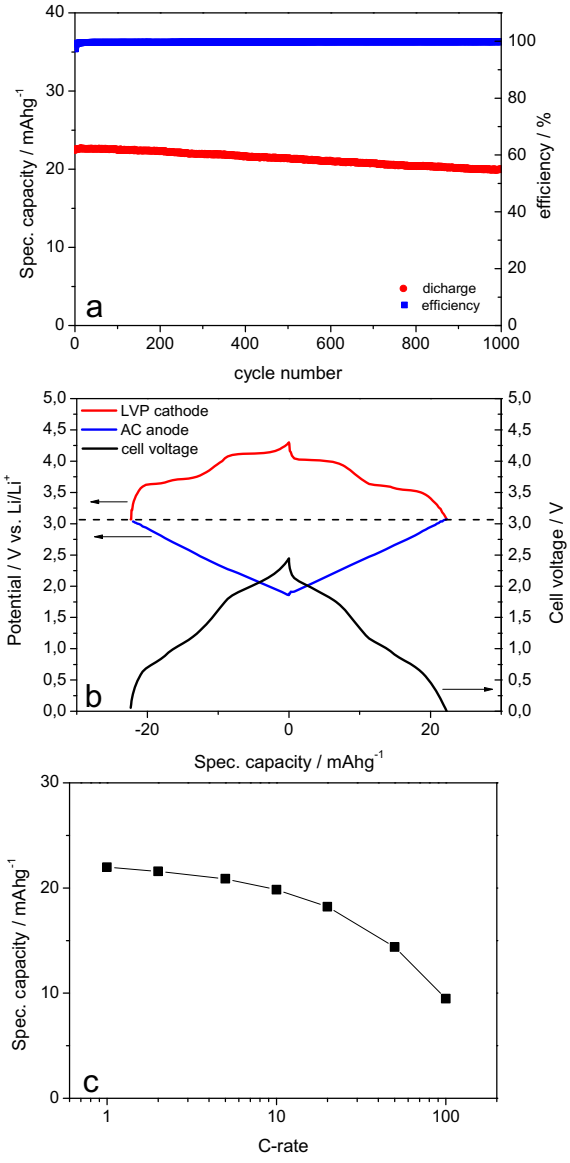

Fig. 4. Hybrid device containing LVP/CA electrode as a cathode and an AC-based anode: (a) long-term cycle performance during CC test carried out at the current density of 0.3 A g^{-1} (corresponding to 10 C); (b) voltage profile of the device in the 10th cycle; (c) rate performance of the device in the range of current densities comprise from 0.03 A g^{-1} to 3.0 A g^{-1}.

be further improved. Nevertheless, these results can be seen as a proof of concept of the use LVP in such hybrid devices.

Fig. 5 shows the performance displayed by a LIC containing an AC cathode combined with a LVP/CA + OA anode. Since no lithium was initially present inside this system, the LVP/CA + OA electrode was pre-lithiated using a protocol similar to that reported in Ref. [41] prior to the CC test (see Electrode preparation and characterization). Similar pre-lithiation processes are also necessary for all LIC containing graphite, and they have been already described in literature [27]. After the pre-lithiation, 1000 full charge–discharge cycles were carried out using a current density corresponding to 10 C (based on the nominal capacity of the LVP/CA + OA anode). Although this LIC loses about 20% of its initial discharge capacity during the first 200 cycles (from about 55 mAh g^{-1} to ca. 42 mAh g^{-1}), the specific capacity stabilizes afterward. At the end of the cycling this LIC delivered a capacity of

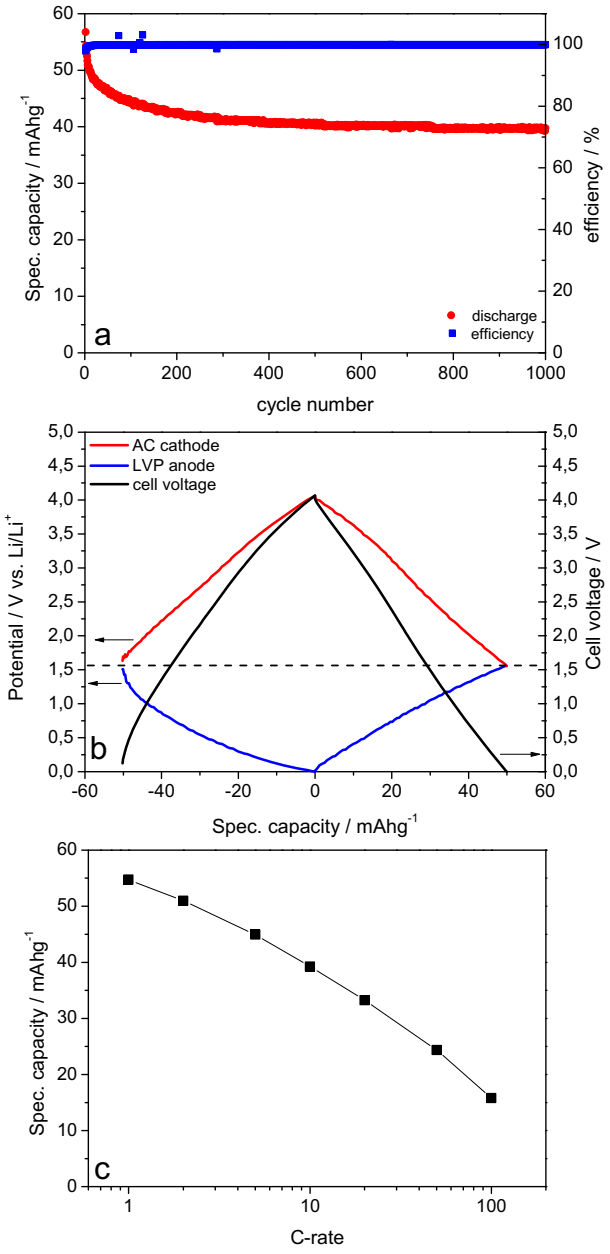

Fig. 5. Lithium-ion capacitor containing LVP/CA + OA electrode as a anode and an AC-based cathode: (a) long-term cycle performance during CC test carried out at the current density of 1.7 A g^{-1} (corresponding to 10 C); (b) voltage profile of the device in the 10th cycle; (c) rate performance of the device in the range of current densities comprise from 0.17 A g^{-1} to 17.0 A g^{-1}.

39.6 mAh g^{-1} (referred to the total active material). In Fig. 5b the voltage profile of the lithium-ion capacitor at the 10th cycle is depicted. As shown, this device displays a maximum cell voltage of 4.0 V, which is a value significantly higher compared to the previous hybrid device. As visible in the figure, the LVP/CA + OA electrode is working in the potential range between 0.0 and 1.5 V. This potential range is smaller compared to the range investigated above, but it has the advantage to make possible a rather large potential excursion for the AC cathode. Since the specific capacity of an AC electrode is linearly dependent on the electrode voltage excursion, a wide potential range is desirable to maximize the delivered capacity of this kind of electrode [42]. Fig. 4c shows the rate capability of this device. As shown, at a current density corresponding to 1 C this LIC delivers 55 mAh g^{-1}. At a current density corresponding to 10 C the device delivers 39 mAh g^{-1}, and even at current density corresponding to 100 C is able to deliver about 16 mAh g^{-1}. It this interesting to note that, although the specific capacity at 100 C is only 29% of the value at 1 C, the absolute value is still significantly higher than the specific capacity of the hybrid device containing LVP/CA at the same C-rate. Considering these results, the cycling stability of this innovative LIC needs certainly to be improved. Nevertheless, these results can be seen as a proof of concept of the use LVP in LIC.

In order to demonstrate the feasibility of a LIB containing cathode and anode both based on LVP, a full cell was realized using the electrode LVP/CA as cathode and the electrode LVP/CA + OA as anode. Initially, different anode/cathode ratios were considered, and a weight ratio LVP/CA + OA/LVP/CA (1:2) was identified as the best one. Therefore, it was used for the realization of the LVP-based

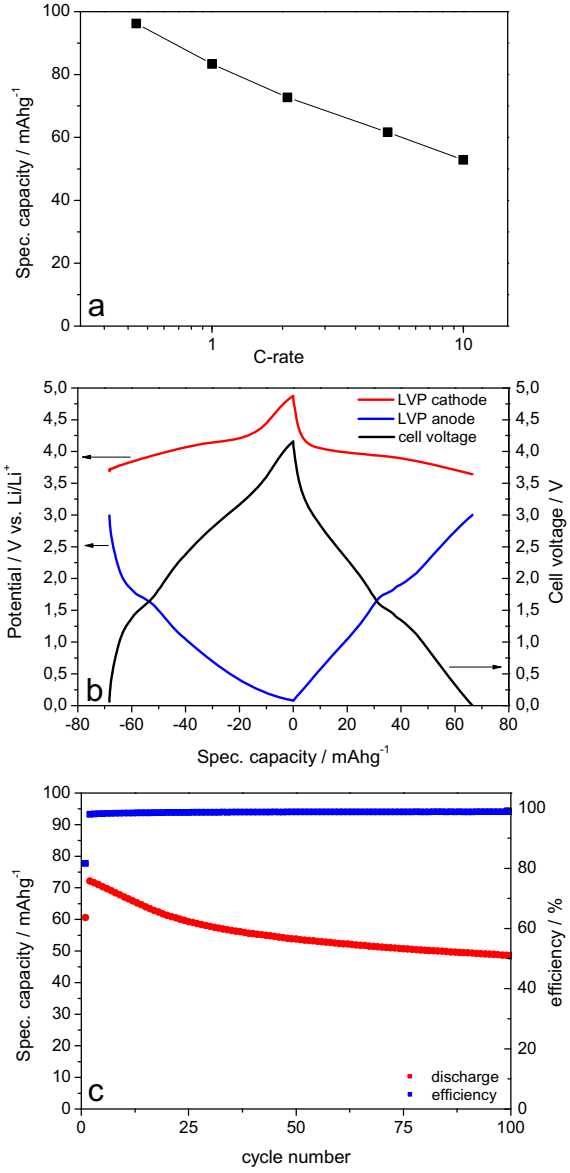

Fig. 6. Lithium-ion battery containing LVP/CA + OA electrode as anode and LVP/CA electrode as cathode: (a) rate performance of the device in the range of current densities comprise from 0.09 A g^{-1} to 1.7 A g^{-1}; (b) voltage profile of the device in the 35th cycle of the cycling test; (c) long-term cycle performance during CC test carried out at the current density of 1.7 A g^{-1} (corresponding to 10 C).

LIB. In the case of this LIB, we initially carried out tests at different C-rates. As shown in Fig. 6a, during charge–discharge carried out at C/2 and 2 C the LIB delivered a capacity of 96 mAh g^{-1} and 74 mAh g^{-1}, respectively (both values are referred to the total active material). At 10 C the LIB delivered 53 mAh g^{-1}, which is 55% of the capacity delivered at C/2. After this test, the LIB was 100 charge–discharge cycles were carried out. As shown in Fig. 6b, such LIB delivers an initial capacity of 72.1 mAh g^{-1} (based the weight of the active materials of both electrodes). However, the capacity fading in the first 25 cycles was rather strong, leading to capacity retention of only 67% after 100 charge–discharge cycles. Fig. 6c shows the cell voltage profile of the as well as the profiles of the cathode and of the anode in the 35th cycle of the cycling test. In order to prevent the LVP/CA + OA anode from entering the potential region of the cathode plateaus, the potential range for the anode is limited to 0.0–3.0 V. As shown, in such LIB the LVP/CA cathode is active in the potential region above 3.0–4.8 V, and therefore the highest of the available LVP plateaus is accessed. The maximum cell voltage, as calculated from the difference between anode and cathode, is about 4.8 V. The performance of such LIB needs to improved, particularly in term of cycling stability, but in our opinion it can be considered promising, particularly when the delivered capacity at 10 C is considered.

Fig. 7 compares in a Ragone-like plot the average energy and power of the three devices considered above. As shown, the system with the lowest specific power and energy is the hybrid device containing LVP/CA as a cathode. When a current density of 0.3 A g^{-1} (corresponding to 10 C) is applied, the device displays average energy and power of 22.1 Wh kg^{-1} and 0.3 kW kg^{-1}, respectively. The performance of this device is limited by its low potential difference between LVP/CA cathode and activated carbon electrode. However, such device displays high cycling stability and, since the cathode is fully lithiated, it does not require any pre-lithiation process before use. The system with the highest performance is the LIC containing the LVP/CA + OA electrode as anode. When a current density of 1.7 A g^{-1} (corresponding to 10 C) is applied, such LIC provides average energy and power of 76.3 Wh kg^{-1} and 3.2 kW kg^{-1}, respectively. The high performance of this device is due to the higher voltage as well as the higher capacity of its electrodes. In order to be used, a pre-lithiation process is needed for this LIC. Nevertheless, we showed that if a proper pre-lithiation step is carried out, such a LIC can displays very high performance. As mentioned above, the C-rate test for the LVP-based battery was carried out before the cycling test and for this reason they are not really comparable with those of the two hybrid devices. Nevertheless, they can be considered as indicative values. As shown in the figure, this battery is able to deliver high specific energy. When a current density of 1.7 A g^{-1} (corresponding to 10 C) is applied, such LIB delivers and average energy and power of 60 Wh kg^{-1} and 3 kW kg^{-1}, respectively. Considering that such LIB needs to further optimize, these values appear certainly promising.

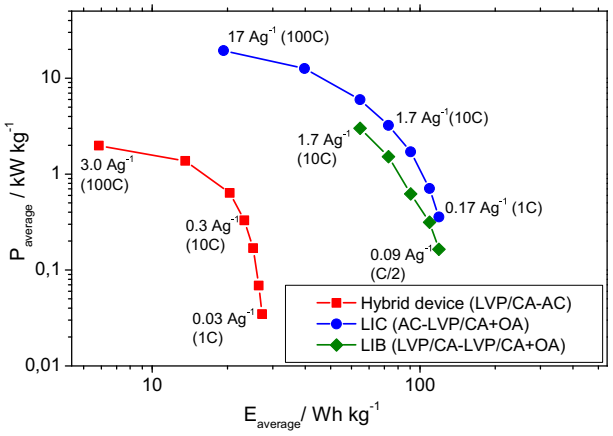

Fig. 7. Comparison of the average energies and power of the hybrid device containing LVP/CA electrode as a cathode, the LIC containing LVP/CA + OA electrode as a anode and the LIB containing LVP/CA + OA electrode as anode and LVP/CA electrode as cathode.

4. Conclusion

The amphoteric character of LVP, together with its high performance at high current densities, makes this material an interesting and flexible candidate for the realization of electrochemical devices. Although LVP is capable to act as cathode and anode material it is important to select the proper LVP-carbon composite in order to access high capacity and ensure cycling stability. However, if a careful selection is made, LVP electrodes can be successfully used in different electrochemical devices. The performance of all the devices presented in this work needs to be improved, nevertheless, the results of our study indicated LVP as a very interesting material for the realization of high-power devices. Moreover, this study demonstrates that it is also possible to realize LIB containing LVP as the only active material. This LIB displays high voltage and very interesting performance during tests carried out at high current density.

Acknowledgments

The authors wish to thank the University of Münster, the Ministry of Innovation, Science and Research of North Rhine-Westphalia (MIWF) within the project “Superkondensator und Lithium-Ionen-Hybrid-Superkondensatoren auf der Basis ionischer Flüssigkeiten” for the financial support.

References

[1] M. Armand, J.M. Tarascon, Nature 451 (2008) 652–657.
[2] D. Larcher, S. Beattie, M. Morcrette, K. Edström, J.C. Jumas, J.M. Tarascon, Journal of Materials Chemistry 17 (2007) 3759–3772.
[3] A.K. Shukla, T. Prem Kumar, Current Science 94 (2008) 314–331.
[4] J.W. Fergus, Journal of Power Sources 195 (2010) 939–954.
[5] W.-J. Zhang, Journal of Power Sources 196 (2011) 13–24.
[6] C. de las Casas, W. Li, Journal of Power Sources 208 (2012) 74–85.
[7] M.Y. Saïdi, J. Barker, H. Huang, J.L. Swoyer, G. Adamson, Journal of Power Sources 119–121 (2003) 266–272.
[8] P. Fu, Y. Zhao, Y. Dong, X. An, G. Shen, Electrochimica Acta 52 (2006) 1003–1008.
[9] Q. Kuang, Y. Zhao, X. An, J. Liu, Y. Dong, L. Chen, Electrochimica Acta 55 (2010) 1575–1581.
[10] M. Ren, Z. Zhou, Y. Li, X.P. Gao, J. Yan, Journal of Power Sources 162 (2006) 1357–1362.
[11] X.H. Rui, N. Yesibolati, C.H. Chen, Journal of Power Sources 196 (2011) 2279–2282.
[12] B. Huang, X. Fan, X. Zheng, M. Lu, Journal of Alloys and Compounds 509 (2011) 4765–4768.
[13] C. Dai, Z. Chen, H. Jin, X. Hu, Journal of Power Sources 195 (2010) 5775–5779.
[14] C. Chang, J. Xiang, X. Shi, X. Han, L. Yuan, J. Sun, Electrochimica Acta 54 (2008) 623–627.
[15] M.M. Ren, Z. Zhou, X.P. Gao, W.X. Peng, J.P. Wei, Journal of Physical Chemistry C 112 (2008) 5689–5693.
[16] X.J. Zhu, Y.X. Liu, L.M. Geng, L.B. Chen, Journal of Power Sources 184 (2008) 578–582.
[17] S. Zhang, Q. Wu, C. Deng, F.L. Liu, M. Zhang, F.L. Meng, H. Gao, Journal of Power Sources 218 (2012) 56–64.
[18] X.H. Rui, C. Li, C.H. Chen, Electrochimica Acta 54 (2009) 3374–3380.
[19] S. Liu, S. Li, K. Huang, Z. Chen, Acta Physico-Chimica Sinica 23 (2007) 537–542.
[20] C. Chang, J. Xiang, X. Shi, X. Han, L. Yuan, J. Sun, Electrochimica Acta 53 (2008) 2232–2237.
[21] P. Fu, Y. Zhao, X. An, Y. Dong, X. Hou, Electrochimica Acta 52 (2007) 5281–5285.
[22] Q. Kuang, Y. Zhao, Journal of Power Sources 216 (2012) 33–35.
[23] X.H. Rui, N. Ding, J. Liu, C. Li, C.H. Chen, Electrochimica Acta 55 (2010) 2384–2390.

[24] X.H. Rui, N. Yesibolati, S.R. Li, C.C. Yuan, C.H. Chen, Solid State Ionics 187 (2011) 58–63.
[25] L. Wang, L.-C. Zhang, I. Lieberwirth, H.-W. Xu, C.-H. Chen, Electrochemistry Communications 12 (2010) 52–55.
[26] H. Olivier-Bourbigou, L. Magna, D. Morvan, Applied Catalysis A: General 373 (2010) 1–56.
[27] V. Khomenko, E. Raymundo-Piñero, F. Béguin, Journal of Power Sources 177 (2008) 643–651.
[28] A. Yoshino, T. Tsubata, M. Shimoyamada, H. Satake, Y. Okano, S. Mori, S. Yata, Journal of the Electrochemical Society 151 (2004) A2180–A2182.
[29] T. Aida, K. Yamada, M. Morita, Electrochemical and Solid-State Letters 9 (2006) 534–536.
[30] H. Li, L. Cheng, Y. Xia, Electrochemical and Solid-State Letters 8 (2005) A433–A436.
[31] J.H. Yoon, H.J. Bang, J. Prakash, Y.K. Sun, Materials Chemistry and Physics 110 (2008) 222–227.
[32] R. Vasanthi, D. Kalpana, N.G. Renganathan, Journal of Solid State Electrochemistry 12 (2008) 961–969.
[33] C.V. Rao, B. Rambabu, Solid State Ionics 181 (2010) 839–843.
[34] H. Wang, M. Yoshio, Electrochemistry Communications 8 (2006) 1481–1486.
[35] D. Cericola, R. Kötz, Electrochimica Acta 72 (2012) 1–17.
[36] N. Böckenfeld, T. Placke, M. Winter, S. Passerini, A. Balducci, Electrochimica Acta 76 (2012) 130–136.
[37] A. Krause, A. Balducci, Electrochemistry Communications 13 (2011) 814–817.
[38] S.B. Tang, M.O. Lai, L. Lu, Journal of Alloys and Compounds 449 (2008) 300–303.
[39] L.R. Faulkner, A.J. Bard, Electrochemical Methods, second ed., Wiley, New York, 2001.
[40] P. Delahay, Journal of the American Chemical Society 75 (1953) 1190–1196.
[41] M. Schroeder, M. Winter, S. Passerini, A. Balducci, Journal of the Electrochemical Society 159 (2012) A1240–A1245.
[42] J.P. Zheng, Journal of the Electrochemical Society 150 (2003) A484–A492.